

Disentangling centrality bias and final-state effects in the production of high- p_T neutral pions using direct photons in d +Au collisions at $\sqrt{s_{NN}} = 200$ GeV

N.J. Abdulameer,^{14,22} U. Acharya,¹⁹ C. Aidala,⁴⁰ Y. Akiba,^{54,55,*} M. Alfred,²¹ K. Aoki,³¹ N. Apadula,²⁷ C. Ayuso,⁴⁰ V. Babintsev,²³ K.N. Barish,⁸ S. Bathe,^{5,55} A. Bazilevsky,⁷ R. Belmont,^{11,47} A. Berdnikov,⁵⁷ Y. Berdnikov,⁵⁷ L. Bichon,⁶⁶ B. Blankenship,⁶⁶ D.S. Blau,^{33,44} M. Boer,³⁵ J.S. Bok,⁴⁶ V. Borisov,⁵⁷ M.L. Brooks,³⁵ J. Bryslawskij,^{5,8} V. Bumazhnov,²³ C. Butler,¹⁹ S. Campbell,¹² V. Canoa Roman,⁶⁰ M. Chiu,⁷ M. Connors,^{19,55} R. Corliss,⁶⁰ Y. Corrales Morales,³⁵ M. Csanád,¹⁵ T. Csörgő,^{39,68} L. D. Liu,⁵¹ T.W. Danley,⁴⁸ M.S. Daugherty,¹ G. David,^{7,60} C.T. Dean,³⁵ K. DeBlasio,⁴⁵ K. Dehmelt,⁶⁰ A. Denisov,²³ A. Deshpande,^{55,60} E.J. Desmond,⁷ V. Doomra,⁶⁰ J.H. Do,⁶⁹ A. Drees,⁶⁰ K.A. Drees,⁶ M. Dumancic,⁶⁷ J.M. Durham,³⁵ A. Durum,²³ T. Elder,¹⁹ A. Enokizono,^{54,56} R. Esha,⁶⁰ B. Fadem,⁴² W. Fan,⁶⁰ N. Feege,⁶⁰ M. Finger, Jr.,⁹ M. Finger,⁹ D. Firak,^{14,60} D. Fitzgerald,⁴⁰ S.L. Fokin,³³ J.E. Frantz,⁴⁸ A. Franz,⁷ A.D. Frawley,¹⁸ Y. Fukuda,⁶⁴ C. Gal,⁶⁰ P. Garg,^{3,60} H. Ge,⁶⁰ M. Giles,⁶⁰ Y. Goto,^{54,55} N. Grau,² S.V. Greene,⁶⁶ T. Gunji,¹⁰ T. Hachiyu,^{43,55} J.S. Haggerty,⁷ K.I. Hahn,¹⁶ S.Y. Han,^{16,32} M. Harvey,⁶² S. Hasegawa,²⁸ T.O.S. Haseler,¹⁹ T.K. Hemmick,⁶⁰ X. He,¹⁹ K. Hill,¹¹ A. Hodges,^{19,24} K. Homma,²⁰ B. Hong,³² T. Hoshino,²⁰ N. Hotvedt,²⁷ J. Huang,⁷ J. Imrek,¹⁴ M. Inaba,⁶⁴ D. Isenhower,¹ Y. Ito,⁴³ D. Ivanishchev,⁵² B.V. Jacak,⁶⁰ Z. Ji,⁶⁰ B.M. Johnson,^{7,19} V. Jorjadze,⁶⁰ D. Jouan,⁵⁰ D.S. Jumper,²⁴ J.H. Kang,⁶⁹ D. Kapukchyan,⁸ S. Karthas,⁶⁰ A.V. Kazantsev,³³ V. Khachatryan,⁶⁰ A. Khanzadeev,⁵² A. Khatiwada,³⁵ C. Kim,^{8,32} D.J. Kim,³⁰ E.-J. Kim,²⁹ M. Kim,⁵⁸ M.H. Kim,³² T. Kim,¹⁶ D. Kincses,¹⁵ A. Kingan,⁶⁰ E. Kistenev,⁷ T. Koblesky,¹¹ D. Kotov,^{52,57} L. Kovacs,¹⁵ S. Kudo,⁶⁴ B. Kurgyis,^{15,60} K. Kurita,⁵⁶ J.G. Lajoie,²⁷ E.O. Lallow,⁴² D. Larionova,⁵⁷ A. Lebedev,²⁷ S.H. Lee,^{27,40,60} M.J. Leitch,³⁵ Y.H. Leung,⁶⁰ N.A. Lewis,⁴⁰ S.H. Lim,^{35,53} M.X. Liu,³⁵ X. Li,³⁵ V.-R. Loggins,²⁴ D.A. Loomis,⁴⁰ D. Lynch,⁷ S. Lökös,³⁹ T. Majoros,¹⁴ M. Makek,⁷⁰ M. Malaev,⁵² V.I. Manko,³³ E. Mannel,⁷ H. Masuda,⁵⁶ M. McCumber,³⁵ D. McGlinchey,^{11,35} A.C. Mignerey,³⁸ D.E. Mihalik,⁶⁰ A. Milov,⁶⁷ D.K. Mishra,⁴ J.T. Mitchell,⁷ M. Mitrnkova,^{57,60} Iu. Mitrnkov,^{57,60} G. Mitsuka,^{31,55} M.M. Mondal,⁶⁰ T. Moon,^{32,69} D.P. Morrison,⁷ S.I. Morrow,⁶⁶ A. Muhammad,⁴¹ B. Mulilo,^{32,54,71} T. Murakami,^{34,54} J. Murata,^{54,56} K. Nagai,⁶³ K. Nagashima,²⁰ T. Nagashima,⁵⁶ J.L. Nagle,¹¹ M.I. Nagy,¹⁵ I. Nakagawa,^{54,55} H. Nakagomi,^{54,64} K. Nakano,^{54,63} C. Nattrass,⁶¹ S. Nelson,¹⁷ R. Nouicer,^{7,55} N. Novitzky,^{60,64} R. Novotny,¹³ T. Novák,^{39,68} G. Nukazuka,^{54,55} A.S. Nyanin,³³ E. O'Brien,⁷ C.A. Ogilvie,²⁷ J. Oh,⁵³ J.D. Orjuela Koop,¹¹ M. Orosz,^{14,22} J.D. Osborn,^{7,40,49} A. Oskarsson,³⁶ K. Ozawa,^{31,64} V. Pantuev,²⁵ V. Papavassiliou,⁴⁶ J.S. Park,⁵⁸ S. Park,^{41,54,58,60} M. Patel,²⁷ S.F. Pate,⁴⁶ W. Peng,⁶⁶ D.V. Perepelitsa,^{7,11} G.D.N. Perera,⁴⁶ C.E. PerezLara,⁶⁰ R. Petti,⁷ M. Phipps,^{7,24} C. Pinkenburg,⁷ M. Potekhin,⁷ A. Pun,⁴⁸ M.L. Purschke,⁷ P.V. Radzevich,⁵⁷ N. Ramasubramanian,⁶⁰ K.F. Read,^{49,61} V. Riabov,^{44,52} Y. Riabov,^{52,57} D. Richford,^{5,65} T. Rinn,^{24,27} M. Rosati,²⁷ Z. Rowan,⁵ J. Runchey,²⁷ T. Sakaguchi,⁷ H. Sako,²⁸ V. Samsonov,^{44,52} M. Sarsour,¹⁹ K. Sato,⁶⁴ S. Sato,²⁸ B. Schaefer,⁶⁶ B.K. Schmoll,⁶¹ R. Seidl,^{54,55} A. Sen,^{27,61} R. Seto,⁸ A. Sexton,³⁸ D. Sharma,⁶⁰ I. Shein,²³ M. Shibata,⁴³ T.-A. Shibata,^{54,63} K. Shigaki,²⁰ M. Shimomura,^{27,43} Z. Shi,³⁵ C.L. Silva,³⁵ D. Silvermyr,³⁶ M. Slunečka,⁹ K.L. Smith,¹⁸ S.P. Sorensen,⁶¹ I.V. Sourikova,⁷ P.W. Stankus,⁴⁹ S.P. Stoll,⁷ T. Sugitate,²⁰ A. Sukhanov,⁷ Z. Sun,^{14,22,60} S. Syed,¹⁹ R. Takahama,⁴³ A. Takeda,⁴³ K. Tanida,^{28,55,58} M.J. Tannenbaum,⁷ S. Tarafdar,^{66,67} A. Taranenko,^{44,59} G. Tarnai,¹⁴ R. Tieulent,^{19,37} A. Timilsina,²⁷ T. Todoroki,^{54,55,64} M. Tomášek,¹³ C.L. Towell,¹ R.S. Towell,¹ I. Tserruya,⁶⁷ Y. Ueda,²⁰ B. Ujvari,^{14,22} H.W. van Hecke,³⁵ S. Vazquez-Carson,¹¹ J. Velkovska,⁶⁶ M. Virius,¹³ V. Vrba,^{13,26} X.R. Wang,^{46,55} Z. Wang,⁵ Y. Watanabe,^{54,55} C.P. Wong,^{19,19,35} C. Xu,⁴⁶ Q. Xu,⁶⁶ Y.L. Yamaguchi,^{55,60} A. Yanovich,²³ P. Yin,¹¹ I. Yoon,⁵⁸ J.H. Yoo,³² I.E. Yushmanov,³³ H. Yu,⁴⁶ W.A. Zajc,¹² and L. Zou⁸

(PHENIX Collaboration)

¹Abilene Christian University, Abilene, Texas 79699, USA

²Department of Physics, Augustana University, Sioux Falls, South Dakota 57197, USA

³Department of Physics, Banaras Hindu University, Varanasi 221005, India

⁴Bhabha Atomic Research Centre, Bombay 400 085, India

⁵Baruch College, City University of New York, New York, New York, 10010 USA

⁶Collider-Accelerator Department, Brookhaven National Laboratory, Upton, New York 11973-5000, USA

⁷Physics Department, Brookhaven National Laboratory, Upton, New York 11973-5000, USA

⁸University of California-Riverside, Riverside, California 92521, USA

⁹Charles University, Faculty of Mathematics and Physics, 180 00 Troja, Prague, Czech Republic

¹⁰Center for Nuclear Study, Graduate School of Science, University of Tokyo, 7-3-1 Hongo, Bunkyo, Tokyo 113-0033, Japan

¹¹University of Colorado, Boulder, Colorado 80309, USA

- ¹²Columbia University, New York, New York 10027 and Nevis Laboratories, Irvington, New York 10533, USA
- ¹³Czech Technical University, Zikova 4, 166 36 Prague 6, Czech Republic
- ¹⁴Debrecen University, H-4010 Debrecen, Egyetem tér 1, Hungary
- ¹⁵ELTE, Eötvös Loránd University, H-1117 Budapest, Pázmány P. s. 1/A, Hungary
- ¹⁶Ewha Womans University, Seoul 120-750, Korea
- ¹⁷Florida A&M University, Tallahassee, FL 32307, USA
- ¹⁸Florida State University, Tallahassee, Florida 32306, USA
- ¹⁹Georgia State University, Atlanta, Georgia 30303, USA
- ²⁰Physics Program and International Institute for Sustainability with Knotted Chiral Meta Matter (WPI-SKCM²), Hiroshima University, Higashi-Hiroshima, Hiroshima 739-8526, Japan
- ²¹Department of Physics and Astronomy, Howard University, Washington, DC 20059, USA
- ²²HUN-REN ATOMKI, H-4026 Debrecen, Bem tér 18/c, Hungary
- ²³IHEP Protvino, State Research Center of Russian Federation, Institute for High Energy Physics, Protvino, 142281, Russia
- ²⁴University of Illinois at Urbana-Champaign, Urbana, Illinois 61801, USA
- ²⁵Institute for Nuclear Research of the Russian Academy of Sciences, prospekt 60-letiya Oktyabrya 7a, Moscow 117312, Russia
- ²⁶Institute of Physics, Academy of Sciences of the Czech Republic, Na Slovance 2, 182 21 Prague 8, Czech Republic
- ²⁷Iowa State University, Ames, Iowa 50011, USA
- ²⁸Advanced Science Research Center, Japan Atomic Energy Agency, 2-4 Shirakata Shirane, Tokai-mura, Naka-gun, Ibaraki-ken 319-1195, Japan
- ²⁹Jeonbuk National University, Jeonju, 54896, Korea
- ³⁰Helsinki Institute of Physics and University of Jyväskylä, P.O.Box 35, FI-40014 Jyväskylä, Finland
- ³¹KEK, High Energy Accelerator Research Organization, Tsukuba, Ibaraki 305-0801, Japan
- ³²Korea University, Seoul 02841, Korea
- ³³National Research Center “Kurchatov Institute”, Moscow, 123098 Russia
- ³⁴Kyoto University, Kyoto 606-8502, Japan
- ³⁵Los Alamos National Laboratory, Los Alamos, New Mexico 87545, USA
- ³⁶Department of Physics, Lund University, Box 118, SE-221 00 Lund, Sweden
- ³⁷IPNL, CNRS/IN2P3, Univ Lyon, Université Lyon 1, F-69622, Villeurbanne, France
- ³⁸University of Maryland, College Park, Maryland 20742, USA
- ³⁹MATE, Institute of Technology, Laboratory of Femtoscopy, Károly Róbert Campus, H-3200 Gyöngyös, Mátrai út 36, Hungary
- ⁴⁰Department of Physics, University of Michigan, Ann Arbor, Michigan 48109-1040, USA
- ⁴¹Mississippi State University, Mississippi State, Mississippi 39762, USA
- ⁴²Muhlenberg College, Allentown, Pennsylvania 18104-5586, USA
- ⁴³Nara Women’s University, Kita-uoya Nishi-machi Nara 630-8506, Japan
- ⁴⁴National Research Nuclear University, MEPhI, Moscow Engineering Physics Institute, Moscow, 115409, Russia
- ⁴⁵University of New Mexico, Albuquerque, New Mexico 87131, USA
- ⁴⁶New Mexico State University, Las Cruces, New Mexico 88003, USA
- ⁴⁷Physics and Astronomy Department, University of North Carolina at Greensboro, Greensboro, North Carolina 27412, USA
- ⁴⁸Department of Physics and Astronomy, Ohio University, Athens, Ohio 45701, USA
- ⁴⁹Oak Ridge National Laboratory, Oak Ridge, Tennessee 37831, USA
- ⁵⁰IPN-Orsay, Univ. Paris-Sud, CNRS/IN2P3, Université Paris-Saclay, BP1, F-91406, Orsay, France
- ⁵¹Peking University, Beijing 100871, People’s Republic of China
- ⁵²PNPI, Petersburg Nuclear Physics Institute, Gatchina, Leningrad region, 188300, Russia
- ⁵³Pusan National University, Pusan 46241, Korea
- ⁵⁴RIKEN Nishina Center for Accelerator-Based Science, Wako, Saitama 351-0198, Japan
- ⁵⁵RIKEN BNL Research Center, Brookhaven National Laboratory, Upton, New York 11973-5000, USA
- ⁵⁶Physics Department, Rikkyo University, 3-34-1 Nishi-Ikebukuro, Toshima, Tokyo 171-8501, Japan
- ⁵⁷Saint Petersburg State Polytechnic University, St. Petersburg, 195251 Russia
- ⁵⁸Department of Physics and Astronomy, Seoul National University, Seoul 151-742, Korea
- ⁵⁹Chemistry Department, Stony Brook University, SUNY, Stony Brook, New York 11794-3400, USA
- ⁶⁰Department of Physics and Astronomy, Stony Brook University, SUNY, Stony Brook, New York 11794-3800, USA
- ⁶¹University of Tennessee, Knoxville, Tennessee 37996, USA
- ⁶²Texas Southern University, Houston, TX 77004, USA
- ⁶³Department of Physics, Tokyo Institute of Technology, Oh-okayama, Meguro, Tokyo 152-8551, Japan
- ⁶⁴Tomonaga Center for the History of the Universe, University of Tsukuba, Tsukuba, Ibaraki 305, Japan
- ⁶⁵United States Merchant Marine Academy, Kings Point, New York 11024, USA
- ⁶⁶Vanderbilt University, Nashville, Tennessee 37235, USA
- ⁶⁷Weizmann Institute, Rehovot 76100, Israel
- ⁶⁸Institute for Particle and Nuclear Physics, HUN-REN Wigner Research Centre for Physics, (HUN-REN Wigner RCP, RMI), H-1525 Budapest 114, POBox 49, Budapest, Hungary
- ⁶⁹Yonsei University, IPAP, Seoul 120-749, Korea
- ⁷⁰Department of Physics, Faculty of Science, University of Zagreb, Bijenička c. 32 HR-10002 Zagreb, Croatia
- ⁷¹Department of Physics, School of Natural Sciences, University of Zambia, Great East Road Campus, Box 32379, Lusaka, Zambia

(Dated: January 17, 2025)

PHENIX presents a simultaneous measurement of the production of direct γ and π^0 in d +Au collisions at $\sqrt{s_{NN}} = 200$ GeV over a p_T range of 7.5 to 18 GeV/ c for different event samples selected by event activity, i.e. charged-particle multiplicity detected at forward rapidity. Direct-photon yields are used to empirically estimate the contribution of hard-scattering processes in the different event samples. Using this estimate, the average nuclear-modification factor, $R_{dAu,EXP}^{\pi^0}$, is $0.925 \pm 0.023(\text{stat}) \pm 0.15(\text{scale})$, consistent with unity for minimum-bias (MB) d +Au collisions. For event classes with low and moderate event activity, $R_{dAu,EXP}^{\pi^0}$ is consistent with the MB value within 5% uncertainty. This result confirms that the previously observed enhancement of high- p_T π^0 production found in small-system collisions with low event activity is a result of a bias in interpreting event activity within the Glauber framework. In contrast, for the top 5% of events with the highest event activity, $R_{dAu,EXP}^{\pi^0}$ is suppressed by 20% relative to the MB value with a significance of 4.5σ , which may be due to final-state effects. This suppression corresponds to a p_T shift of $\delta p_T = 0.213 \pm 0.055$ GeV/ c at 9 GeV/ c .

High transverse-momentum (p_T) particles are produced in rare, initial hard-scattering processes and are sensitive to the evolution of relativistic heavy-ion collisions. The suppression of their yields with respect to the incoherent superposition of yields from p + p collisions was predicted [1–3] as a signature for the formation of a hot and dense partonic medium, the quark-gluon plasma (QGP). This was first observed in A + A collisions at the Relativistic Heavy Ion Collider (RHIC) [4, 5] and later at the Large Hadron Collider (LHC) [6–8]. Together with the absence of suppression in minimum-bias (MB) d +Au [9, 10] collisions at RHIC and p +Pb collisions at the LHC [11, 12], it served as a compelling piece of evidence that QGP is formed in heavy-ion collisions.

Multiparticle correlations [13–18] and strangeness enhancement [19] in collisions of small-on-large nuclei (x + A) with high particle multiplicity, or event activity, have led to the suggestion that QGP droplets may be formed even in small systems. If true, one may also find evidence for energy loss of high- p_T particles in these collisions. However, measurements at RHIC [20, 21] and LHC [22, 23] have revealed an inconclusive pattern of suppression in high-activity events, and a puzzling enhancement in low-activity events.

Theoretical calculations predict that any presence of QGP in x + A collisions should result in a suppression of high- p_T hadrons [24, 25]. While there are now stringent experimental limits on energy loss for jets with p_T above 15 GeV/ c in p +Pb collisions at the LHC [17, 26], the p_T range below 15 GeV/ c remains less constrained, and the cause of the enhancement in low activity events remains unclear. To better understand these observations, high p_T particle production in x + A at RHIC needs to be explored with greater accuracy.

Evidence for energy loss is typically quantified by the nuclear-modification factor, R_{AB} , as a function of p_T :

$$R_{AB}(p_T) = \frac{Y_{AB}(p_T)}{N_{\text{coll}} Y_{pp}(p_T)}, \quad (1)$$

where Y_{AB} and Y_{pp} are the yields in A + B and p + p collisions, respectively, with A and B being large or small

ions. The average number of binary nucleon-nucleon (NN) collisions, N_{coll} is used to scale particle production from hard-scattering processes from p + p to A + B events. Because N_{coll} is not experimentally accessible, the Glauber model (GLM) [27, 28] is usually used to map N_{coll} to the measured event activity or centrality. The basic tenet is that the majority of NN collisions involve only small momentum exchanges; thus, N_{coll} can be estimated with the eikonal approximation.

The observation that the direct photon R_{AA} is consistent with unity in Au+Au collisions, independent of the event selection [29], confirmed that the particle production from hard-scattering processes scales with N_{coll} . Similar behavior has been seen at the LHC for electromagnetic (EM) probes [30–34] including the Z boson [35].

Studies at RHIC and LHC [36–38] indicate that the GLM based mapping of various measures of event activity to N_{coll} can be biased by the presence of hard-scattering processes. The effect will not be noticeable if N_{coll} is large [37], but it can be significant if N_{coll} is small, as in peripheral A + A collisions or collisions of x + A systems [38–42]. In x + A collisions, this bias would manifest itself as an underestimate (overestimate) of N_{coll} for events with low (high) event activity leading to an apparent enhancement (suppression) of high- p_T hadron or jet yields. Although the effect of this selection bias has been studied extensively [43–45], it remains a challenge to disentangle the final-state effects in R_{xA} from the impact of this bias.

This letter aims to resolve the ambiguity of whether the observed enhancement and/or suppression pattern in R_{dAu} for d +Au collisions selected by event activity [21] is due to an event-selection bias in estimating N_{coll} or true nuclear effects. To achieve this, high- p_T direct photons (γ^{dir}) are employed as a benchmark for particle production from hard-scattering processes in a given event sample [46]. They are used to experimentally estimate the number of binary collisions ($N_{\text{coll}}^{\text{EXP}}$) for a given event selection from the ratio of the direct-photon yields in that selection to that from p + p collisions:

$$N_{\text{coll}}^{\text{EXP}}(p_T) = \frac{Y_{d\text{Au}}^{\gamma^{\text{dir}}}(p_T)}{Y_{pp}^{\gamma^{\text{dir}}}(p_T)}. \quad (2)$$

Here it is assumed that final-state effects on photons are negligible. Indeed, in Au+Au collisions, where $R_{AA}^{\gamma^{\text{dir}}}$ is consistent with unity and shows no appreciable p_T dependence [29], $N_{\text{coll}}^{\text{EXP}}$ is equal to N_{coll} as determined by the GLM ($N_{\text{coll}}^{\text{GL}}$). Because cold-nuclear-matter (CNM) effects on γ^{dir} in d +Au are expected to be similar or smaller than in Au+Au [47], $N_{\text{coll}}^{\text{EXP}}$ is also a measure of N_{coll} in d +Au with the advantage that it is less sensitive to potential event-selection biases than $N_{\text{coll}}^{\text{GL}}$. Theoretical calculations suggest that there are changes in the probability of hard scattering owing to the presence of CNM effects, including differences in isospin, i.e. different u and d quark content in p + p and d +Au collisions, shadowing, the EMC effect, etc. [25, 47, 48]. These are predicted to result in a reduction in the production of high p_T γ^{dir} in d +Au collisions of up to 10% over the p_T range investigated here [47]. The same calculations show a similar decrease in pion production. Accounting for the different Bjorken- x regions spanned by γ^{dir} and π^0 , the p_T dependence of their relative yields between d +Au and p + p collisions cancels within 5%. While these calculations are for MB collisions, they are expected to hold true for all event selections. Compared to the current experimental uncertainties these differences are small, further justifying the use of Eq. 2 to test the scaling of high- p_T particle production from p + p to a given d +Au event sample.

The π^0 and direct-photon data were recorded with the PHENIX experiment [49] in 2016 using a triggered event sample of 12.6×10^6 d +Au collisions, corresponding to an integrated luminosity of ≈ 50 nb $^{-1}$. In addition, a MB data sample of 65×10^6 events is used to define event activity classes, based on the charged particle multiplicity in the Au-going direction, and to determine the absolute normalization of the π^0 and direct photon spectra. The MB trigger requires a coincidence of at least one hit in the upstream and downstream beam-beam Counters [50] (covering the pseudorapidity range $3.0 < |\eta| < 3.9$), which records $88 \pm 4\%$ of the inelastic cross section. The event trigger required a local energy deposit (> 2.4 GeV) in the electromagnetic calorimeter [51] (EMCal, $|\eta| < 0.35$).

The π^0 mesons are reconstructed using the $\pi^0 \rightarrow \gamma\gamma$ decay as described in [5, 52]. Photon candidates are identified by comparing the shape and timing of the reconstructed energy clusters to the expected response of the EMCal. All photon candidates in an event are combined into pairs, their invariant mass is calculated, and the mass distribution is aggregated in bins of reconstructed p'_T . Any combinatorial background is subtracted. The result is the raw π^0 yield, $dN_{\text{raw}}^{\pi^0}/dp'_T$, which is corrected to represent the true π^0 yield, dN^{π^0}/dp_T , in the rapid-

ity range $|y| < 0.5$. The correction is determined by an iterative unfolding procedure similar to the standard Bayesian approach, using a response matrix, $M(p_T, p'_T)$, with elements that are the probability that a π^0 of a given true p_T , uniformly distributed in azimuth and in $|y| < 0.5$, will be reconstructed in PHENIX as a π^0 with p'_T . The simulated response is determined with a GEANT3 [53] implementation of the PHENIX experiment. The yield of photon candidates constitutes the raw inclusive photon yield, $\gamma_{\text{raw}}^{\text{incl}}$, and contains energy clusters from direct photons, clusters from single decay photons, and clusters reconstructed from overlapping EM showers from two decay photons. The direct-photon yield is extracted from the $\gamma_{\text{raw}}^{\text{incl}}$ yield following [5, 29] without isolation requirements. To determine the contribution of decay photons to the raw inclusive yield, two additional response matrices are generated, $M(p_T(\pi^0), p'_T(\gamma))$ and $M(p_T(\eta), p'_T(\gamma))$. Here the elements are the number of photon candidates reconstructed with p'_T for a π^0 (η) of a given p_T . The reconstructed decay photon candidates from π^0 are given by $M(p_T(\pi^0), p'_T(\gamma)) \times dN^{\pi^0}/dp_T$, using the corrected π^0 p_T spectrum.

The contribution from other meson decays is calculated as $M(p_T(\eta), p'_T(\gamma)) \times dN^{\eta}/dp_T \times (1 + \gamma^{\omega, \eta'}/\gamma^{\eta})$. The η meson p_T spectrum is taken as $dN^{\eta}/dp_T = \eta/\pi^0 \times dN^{\pi^0}/dp_T$, using the p_T dependent η/π^0 ratio determined in [54]. The photon candidates from η decays are then scaled by the ratio $\gamma^{\omega, \eta'}/\gamma^{\eta} = 0.19$ to account for the contribution from ω and η' meson decays, which is independent of p_T above 7 GeV/ c [55]. This raw decay-photon contribution to the photon candidates is subtracted from the raw inclusive-photon yield. The remaining photon candidates constitute the raw direct-photon yield, which is corrected using the same iterative method deployed for π^0 [56]. Finally, for each event class, the absolute normalization of π^0 and γ^{dir} yields is corrected for the average p_T independent bias induced by a hard process on $N_{\text{coll}}^{\text{GL}}$ [36].

The systematic uncertainties on the π^0 and γ^{dir} yields are evaluated following established procedures [21]. For d +Au they vary between 11% to 15% over the p_T range from 7.5 to 18 GeV/ c . Sources of uncertainties include the energy scale calibration, the amount of material in the detector where photons convert, the photon shower identification, shower merging, the absolute normalization, plus other smaller contributions. These sources are common to π^0 and γ^{dir} . For γ^{dir} additional uncertainties due to the hadron contamination and the contribution of decay photons from η , ω , and η' are considered. In the $\gamma^{\text{dir}}/\pi^0$ ratio many uncertainties cancel, including uncertainties from normalization, reducing the systematic uncertainties to about 6% to 9% independent of event activity. To assure that there are no event-activity-dependent uncertainties, the corrections for the π^0 and γ^{dir} yields were determined separately for each event class. With exception of the absolute normalization correction, they

are found to be equal within an accuracy of 1% (see supplemental material [57]).

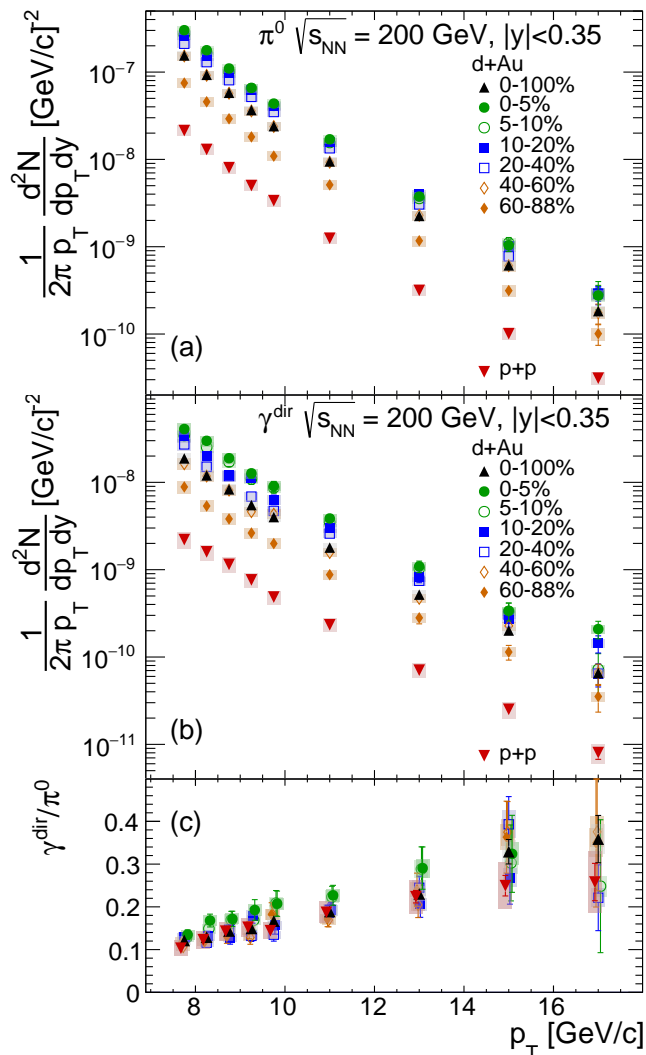


FIG. 1. The p_T distribution at high p_T of (a) neutral pions and (b) direct photons for different $d+Au$ event activity classes compared to those from $p+p$ collisions. Panel (c) shows the ratio $\gamma^{\text{dir}}/\pi^0$. For better visibility the points are slightly shifted in p_T .

Invariant yields of π^0 and γ^{dir} covering the p_T range from 7.5 to 18 GeV/ c are shown in Fig. 1(a) and (b), respectively. Both panels include the yield for $d+Au$ (0%–100%) and for six $d+Au$ event classes selected by event activity, with 0%–5% being the events with the largest activity. Invariant yields measured in $p+p$ [21, 58] are also shown. The $d+Au$ results for π^0 and for MB γ^{dir} are consistent with previous measurements [21, 59]. Fig. 1(c) presents the $\gamma^{\text{dir}}/\pi^0$ ratios. The $\gamma^{\text{dir}}/\pi^0$ ratio for $d+Au$ (0%–100%) is consistent with that from $p+p$ collisions. This is also true for all $d+Au$ event classes with low to moderate event activity. The similarity of $\gamma^{\text{dir}}/\pi^0$ for $p+p$ and most $d+Au$ collisions suggests that initial state

CNM effects must be similar for the production of high- p_T π^0 and γ^{dir} . This supports the conjecture that the earlier observed enhancement of $R_{xA}^{\pi^0}$ in $x+A$ collisions with low event activity [21] was caused by a bias in the mapping of event activity to $N_{\text{coll}}^{\text{GL}}$. In contrast, the $\gamma^{\text{dir}}/\pi^0$ ratio for the $d+Au$ events with high activity (0%–5%) is visibly larger than the one for $p+p$.

To further quantify the bias in mapping event activity to $N_{\text{coll}}^{\text{GL}}$, $N_{\text{coll}}^{\text{EXP}}$ and $N_{\text{coll}}^{\text{GL}}$ are compared directly for the different event classes. Figures 2(a) to (c) show $N_{\text{coll}}^{\text{EXP}}$ versus p_T for MB $d+Au$ events (0%–100%), and those with high (0%–5%) and low (60%–88%) event activity. The figure includes the average values of $N_{\text{coll}}^{\text{EXP}}$ determined from fits to the data (solid lines) compared to $N_{\text{coll}}^{\text{GL}}$ (dashed lines) [55]. The systematic uncertainties on $N_{\text{coll}}^{\text{EXP}}$, $\approx 16\%$, are dominated by uncertainties on the $p+p$ data set and thus are a common scale uncertainty for all $d+Au$ event classes. The $N_{\text{coll}}^{\text{EXP}}$ and $N_{\text{coll}}^{\text{GL}}$ agree well for 0%–100%, and are consistent for all event selections within uncertainties. However, the ratio of $N_{\text{coll}}^{\text{EXP}}/N_{\text{coll}}^{\text{GL}}$ shown in Fig.3(a) has a clear trend with event activity. The ratio is larger than one for events with low activity. The $N_{\text{coll}}^{\text{EXP}}/N_{\text{coll}}^{\text{GL}}$ ratio decreases with increasing activity and becomes consistent with unity. The significance of this trend is evaluated by calculating the double ratio, $N_{\text{coll}}^{\text{EXP}}(i)/N_{\text{coll}}^{\text{EXP}}(0\%–100\%)$ to $N_{\text{coll}}^{\text{GL}}(i)/N_{\text{coll}}^{\text{GL}}(0\%–100\%)$ for the event selection i . For 0%–5% and 60%–88% the double ratio is $0.96 \pm 0.05 \pm 0.01$ and $1.16 \pm 0.07 \pm 0.06$, respectively. The systematic uncertainties mostly cancel so that only the uncertainties on the bias factor remain. Because $N_{\text{coll}}^{\text{GL}}$ and $N_{\text{coll}}^{\text{EXP}}$ agree reasonably well for 0%–100% and events with large event activity, it seems that $N_{\text{coll}}^{\text{GL}}$ underestimates the number of hard scattering processes in events with low event activity. This may have led to the previously observed enhancement of R_{xA} for π^0 in $p+Au$, $d+Au$ and ${}^3\text{He}+Au$ collisions [21].

Next, possible nuclear modifications of π^0 production in $d+Au$ collisions with high event activity are investigated. For this the nuclear modification factor is calculated using $N_{\text{coll}}^{\text{EXP}}$ (as defined in Eq. 2) instead of $N_{\text{coll}}^{\text{GL}}$,

$$R_{dAu,\text{EXP}}^{\pi^0} = \frac{Y_{dAu}^{\pi^0}}{N_{\text{coll}}^{\text{EXP}} Y_{pp}^{\pi^0}} = \frac{Y_{pp}^{\text{dir}}/Y_{pp}^{\pi^0}}{Y_{dAu}^{\text{dir}}/Y_{dAu}^{\pi^0}}, \quad (3)$$

which is equivalent to the double ratio of $\gamma^{\text{dir}}/\pi^0$ ratios. Figures 2(d) to (f) show $R_{dAu,\text{EXP}}^{\pi^0}$ for the same event classes as panels (a) to (c). Over the observed p_T range there is no appreciable p_T dependence; the results of fits to the data are also indicated. Within uncertainties, $R_{dAu,\text{EXP}}^{\pi^0}$ for 0%–100% is consistent with unity. The same is the case for $R_{dAu,\text{EXP}}^{\pi^0}$ from lowest event-activity sample (60%–88%). In contrast, for the highest event activity-sample (0%–5%), a small but significant suppression of $\approx 20\%$ can be seen.

The evolution of the average $R_{dAu,\text{EXP}}^{\pi^0}$ as a function

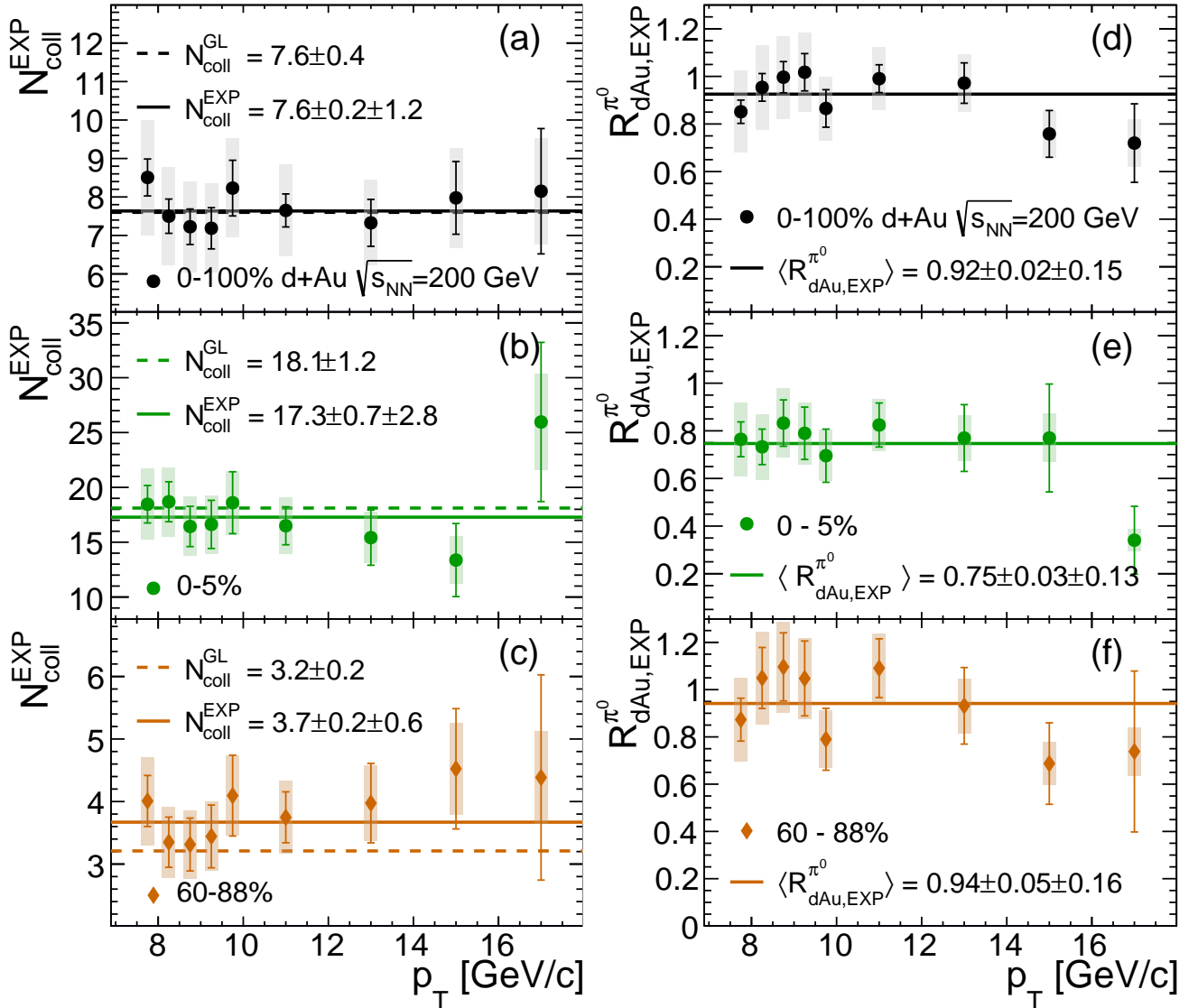


FIG. 2. Values of $N_{\text{coll}}^{\text{EXP}}$ versus p_T as defined in Eq. 2 for three $d+\text{Au}$ event classes, (a) 0%–100%, (b) 0%–5% and (c) 60%–88%. Also shown are fits to the data (solid lines) and the corresponding value $N_{\text{coll}}^{\text{GL}}$ (dashed lines). Panels (d) to (f) show the nuclear modification factors $R_{\text{dAu,EXP}}^{\pi^0}$, calculated with Eq. 3, for the same event selections as in panels (a) to (c) together with fits to the data.

of $N_{\text{coll}}^{\text{EXP}}$ is shown in Fig. 3(b). The points below 14 in $N_{\text{coll}}^{\text{EXP}}$ are consistent with the 0%–100% value, and within the scale uncertainty of 16.5% consistent with unity or a few percent increase above unity, which would be expected from CNM effects [47]. However, for the collisions with the largest event activity $R_{\text{dAu,EXP}}^{\pi^0}$ is significantly reduced. The reduction is quantified by a double ratio in which the systematic uncertainties cancel:

$$\frac{R_{\text{dAu,EXP}}^{\pi^0}(0\%-5\%)}{R_{\text{dAu,EXP}}^{\pi^0}(0\%-100\%)} = 0.806 \pm 0.042, \quad (4)$$

with a 4.5σ deviation from unity. The same ratio for the events with the smallest event activity is 1.017 ± 0.056 ,

consistent with unity. The observed 0.806 ± 0.042 suppression of the π^0 yield corresponds to a p_T shift of $\delta p_T = 0.213 \pm 0.055$ GeV/c at 9 GeV/c. This shift is smaller than upper limits currently set by LHC experiments [17, 26]. energy loss was limited to 0.4 GeV/c outside of a cone of $R = 0.4$ for 15 GeV/c jets from $p+\text{Pb}$ collisions [17]. These limits suggest that the LHC measurement would not be sensitive to the suppression observed here. Multiple factors increase the sensitivity of PHENIX, including (i) experimental techniques, such as eliminating any model dependence, minimizing systematic uncertainties through double ratios, and choosing a larger system, (ii) the softer momentum spectrum

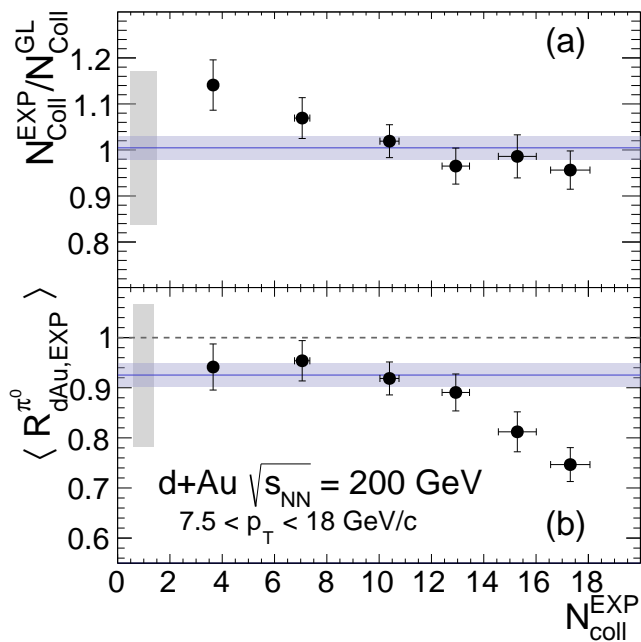


FIG. 3. The ratio (a) $N_{\text{coll}}^{\text{EXP}}/N_{\text{coll}}^{\text{GL}}$ and (b) the average $R_{d\text{Au},\text{EXP}}^{\pi^0}$ as a function of $N_{\text{coll}}^{\text{EXP}}$. Horizontal and vertical bars are the statistical uncertainties. The values for 0%–100% centrality $d+\text{Au}$ collisions are represented by a solid [blue] line, with the statistical uncertainty given as a band. The scale uncertainties that are common to all data points are shown for the 0%–100% value.

at RHIC compared to at the LHC, and (iii) measuring leading particles rather than partial jet energies.

In summary, with the simultaneous measurement of π^0 and γ^{dir} at high p_{T} in $d+\text{Au}$ collisions at $\sqrt{s_{\text{NN}}} = 200$ GeV, PHENIX has established that the previously observed enhancement of $\pi^0 R_{d\text{Au}}$ in events with low activity is likely caused by an event-selection bias in estimating $N_{\text{coll}}^{\text{GL}}$ within the GLM framework. The $N_{\text{coll}}^{\text{EXP}}$ based on direct photons, introduced in this paper, provides a more accurate approximation of the hard-scattering contribution. Using $N_{\text{coll}}^{\text{EXP}}$ eliminates the enhancement, while maintaining a 20% suppression of high p_{T} π^0 in events with high activity. The observed suppression is qualitatively consistent with the predictions of energy loss in small systems [24, 25]. If the suppression is indeed due to hot-matter effects, the yield of fragmentation photons within γ^{dir} may also be suppressed, which in turn would lead to a slight underestimate of the suppression. To the contrary, any remaining bias in the event selection, for example due to the different Bjorken- x range sampled by events with γ^{dir} or π^0 with the same p_{T} , could add to the suppression. Further studies of the system-size dependence with $p+\text{Au}$, $d+\text{Au}$, and $^3\text{He}+\text{Au}$ collisions may shed more light on the origin of the observed suppression.

We thank the staff of the Collider-Accelerator and Physics Departments at Brookhaven National Labora-

tory and the staff of the other PHENIX participating institutions for their vital contributions. We acknowledge support from the Office of Nuclear Physics in the Office of Science of the Department of Energy, the National Science Foundation, Abilene Christian University Research Council, Research Foundation of SUNY, and Dean of the College of Arts and Sciences, Vanderbilt University (U.S.A), Ministry of Education, Culture, Sports, Science, and Technology and the Japan Society for the Promotion of Science (Japan), Natural Science Foundation of China (People’s Republic of China), Croatian Science Foundation and Ministry of Science and Education (Croatia), Ministry of Education, Youth and Sports (Czech Republic), Centre National de la Recherche Scientifique, Commissariat à l’Énergie Atomique, and Institut National de Physique Nucléaire et de Physique des Particules (France), J. Bolyai Research Scholarship, EFOP, the New National Excellence Program (ÚNKP), NKFIH, and OTKA (Hungary), Department of Atomic Energy and Department of Science and Technology (India), Israel Science Foundation (Israel), Basic Science Research and SRC(CENuM) Programs through NRF funded by the Ministry of Education and the Ministry of Science and ICT (Korea). Ministry of Education and Science, Russian Academy of Sciences, Federal Agency of Atomic Energy (Russia), VR and Wallenberg Foundation (Sweden), University of Zambia, the Government of the Republic of Zambia (Zambia), the U.S. Civilian Research and Development Foundation for the Independent States of the Former Soviet Union, the Hungarian American Enterprise Scholarship Fund, the US-Hungarian Fulbright Foundation, and the US-Israel Binational Science Foundation.

* PHENIX Spokesperson: akiba@rcf.rhic.bnl.gov

- [1] X.-N. Wang and M. Gyulassy, Gluon shadowing and jet quenching in A+A collisions at $\sqrt{s} = 200\text{GeV}$, Phys. Rev. Lett. **68**, 1480 (1992).
- [2] X.-N. Wang, Effect of jet quenching on high p_{T} hadron spectra in high-energy nuclear collisions, Phys. Rev. C **58**, 2321 (1998).
- [3] M. Gyulassy, P. Levai, and I. Vitev, NonAbelian energy loss at finite opacity, Phys. Rev. Lett. **85**, 5535 (2000).
- [4] K. Adcox *et al.* (PHENIX Collaboration), Suppression of hadrons with large transverse momentum in central Au+Au collisions at $\sqrt{s_{\text{NN}}} = 130$ GeV, Phys. Rev. Lett. **88**, 022301 (2002).
- [5] A. Adare *et al.* (PHENIX Collaboration), Suppression pattern of neutral pions at high transverse momentum in Au+Au collisions at $\sqrt{s_{\text{NN}}} = 200$ GeV and constraints on medium transport coefficients, Phys. Rev. Lett. **101**, 232301 (2008).
- [6] B. Abelev *et al.* (ALICE Collaboration), Centrality Dependence of Charged Particle Production at Large Transverse Momentum in Pb-Pb Collisions at $\sqrt{s_{\text{NN}}} = 2.76$ TeV, Phys. Lett. B **720**, 52 (2013).

- [7] G. Aad *et al.* (ATLAS Collaboration), Measurement of charged-particle spectra in Pb+Pb collisions at $\sqrt{s_{NN}} = 2.76$ TeV with the ATLAS detector at the LHC, *J. High Energy Phys.* **09**, 050 (2015).
- [8] V. Khachatryan *et al.* (CMS Collaboration), Nuclear Effects on the Transverse Momentum Spectra of Charged Particles in pPb Collisions at $\sqrt{s_{NN}} = 5.02$ TeV, *Eur. Phys. J. C* **75**, 237 (2015).
- [9] S. S. Adler *et al.* (PHENIX Collaboration), Absence of suppression in particle production at large transverse momentum in $\sqrt{s_{NN}} = 200$ GeV d+Au collisions, *Phys. Rev. Lett.* **91**, 072303 (2003).
- [10] J. Adams *et al.* (STAR Collaboration), Evidence from d+Au measurements for final state suppression of high p_T hadrons in Au+Au collisions at RHIC, *Phys. Rev. Lett.* **91**, 072304 (2003).
- [11] B. Abelev *et al.* (ALICE Collaboration), Transverse momentum distribution and nuclear modification factor of charged particles in p-Pb collisions at $\sqrt{s_{NN}} = 5.02$ TeV, *Phys. Rev. Lett.* **110**, 082302 (2013).
- [12] V. Khachatryan *et al.* (CMS Collaboration), Charged-particle nuclear modification factors in PbPb and pPb collisions at $\sqrt{s_{NN}} = 5.02$ TeV, *J. High Energy Phys.* **04**, 039 (2017).
- [13] B. B. Abelev *et al.* (ALICE Collaboration), Multiparticle azimuthal correlations in p-Pb and Pb-Pb collisions at the CERN Large Hadron Collider, *Phys. Rev. C* **90**, 054901 (2014).
- [14] A. Adare *et al.* (PHENIX Collaboration), Measurement of long-range angular correlation and quadrupole anisotropy of pions and (anti)protons in central d+Au collisions at $\sqrt{s_{NN}}=200$ GeV, *Phys. Rev. Lett.* **114**, 192301 (2015).
- [15] V. Khachatryan *et al.* (CMS Collaboration), Evidence for Collective Multiparticle Correlations in p-Pb Collisions, *Phys. Rev. Lett.* **115**, 012301 (2015).
- [16] V. Khachatryan *et al.* (CMS Collaboration), Evidence for collectivity in pp collisions at the LHC, *Phys. Lett. B* **765**, 193 (2017).
- [17] S. Acharya *et al.* (ALICE Collaboration), Constraints on jet quenching in p-Pb collisions at $\sqrt{s_{NN}} = 5.02$ TeV measured by the event-activity dependence of semi-inclusive hadron-jet distributions, *Phys. Lett. B* **783**, 95 (2018).
- [18] C. Aidala *et al.* (PHENIX Collaboration), Creation of quark-gluon plasma droplets with three distinct geometries, *Nature Phys.* **15**, 214 (2019).
- [19] J. Adam *et al.* (ALICE Collaboration), Enhanced production of multi-strange hadrons in high-multiplicity proton-proton collisions, *Nature Phys.* **13**, 535 (2017).
- [20] M. G. Wysocki (PHENIX Collaboration), Cold nuclear matter effects at PHENIX, *Nucl. Phys. A* **904-905**, 67c (2013).
- [21] U. A. Acharya *et al.* (PHENIX Collaboration), Systematic study of nuclear effects in p +Al, p +Au, d +Au, and $^3\text{He} + \text{Au}$ collisions at $\sqrt{s_{NN}} = 200$ GeV using π^0 production, *Phys. Rev. C* **105**, 064902 (2022).
- [22] G. Aad *et al.* (ATLAS Collaboration), Centrality and rapidity dependence of inclusive jet production in $\sqrt{s_{NN}} = 5.02$ TeV proton-lead collisions with the ATLAS detector, *Phys. Lett. B* **748**, 392 (2015).
- [23] G. Aad *et al.* (ATLAS Collaboration), Transverse momentum, rapidity, and centrality dependence of inclusive charged-particle production in $\sqrt{s_{NN}} = 5.02$ TeV p+Pb collisions measured by the ATLAS experiment, *Phys. Lett. B* **763**, 313 (2016).
- [24] A. Huss, A. Kurkela, A. Mazeliauskas, R. Paatelainen, W. van der Schee, and U. A. Wiedemann, Predicting parton energy loss in small collision systems, *Phys. Rev. C* **103**, 054903 (2021).
- [25] W. Ke and I. Vitev, Searching for QGP droplets with high-pT hadrons and heavy flavor, *Phys. Rev. C* **107**, 064903 (2023).
- [26] G. Aad *et al.* (ATLAS Collaboration), Strong Constraints on Jet Quenching in Centrality-Dependent p+Pb Collisions at 5.02 TeV from ATLAS, *Phys. Rev. Lett.* **131**, 072301 (2023).
- [27] R. J. Glauber and G. Matthiae, High-energy scattering of protons by nuclei, *Nucl. Phys. B* **21**, 135 (1970).
- [28] M. L. Miller, K. Reygers, S. J. Sanders, and P. Steinberg, Glauber modeling in high energy nuclear collisions, *Ann. Rev. Nucl. Part. Sci.* **57**, 205 (2007).
- [29] S. Afanasiev *et al.* (PHENIX Collaboration), Measurement of Direct Photons in Au+Au Collisions at $\sqrt{s_{NN}} = 200$ GeV, *Phys. Rev. Lett.* **109**, 152302 (2012).
- [30] S. Chatrchyan *et al.* (CMS Collaboration), Measurement of isolated photon production in pp and PbPb collisions at $\sqrt{s_{NN}} = 2.76$ TeV, *Phys. Lett. B* **710**, 256 (2012).
- [31] J. Adam *et al.* (ALICE Collaboration), Direct photon production in Pb-Pb collisions at $\sqrt{s_{NN}} = 2.76$ TeV, *Phys. Lett. B* **754**, 235 (2016).
- [32] G. Aad *et al.* (ATLAS Collaboration), Centrality, rapidity and transverse momentum dependence of isolated prompt photon production in lead-lead collisions at $\sqrt{s_{NN}} = 2.76$ TeV measured with the ATLAS detector, *Phys. Rev. C* **93**, 034914 (2016).
- [33] G. Aad *et al.* (ATLAS Collaboration), Z boson production in Pb+Pb collisions at $\sqrt{s_{NN}}= 5.02$ TeV measured by the ATLAS experiment, *Phys. Lett. B* **802**, 135262 (2020).
- [34] A. M. Sirunyan *et al.* (CMS Collaboration), Constraints on the Initial State of Pb-Pb Collisions via Measurements of Z-Boson Yields and Azimuthal Anisotropy at $\sqrt{s_{NN}}=5.02$ TeV, *Phys. Rev. Lett.* **127**, 102002 (2021).
- [35] There is some disagreement between ATLAS and CMS in event classes with low activity where N_{coll} is small and the events are categorized in a different way.
- [36] A. Adare *et al.* (PHENIX Collaboration), Centrality categorization for $R_{p(d)+A}$ in high-energy collisions, *Phys. Rev. C* **90**, 034902 (2014).
- [37] J. Adam *et al.* (ALICE Collaboration), Centrality dependence of particle production in p-Pb collisions at $\sqrt{s_{NN}}= 5.02$ TeV, *Phys. Rev. C* **91**, 064905 (2015).
- [38] M. Kordell and A. Majumder, Jets in d(p)-A Collisions: Color Transparency or Energy Conservation, *Phys. Rev. C* **97**, 054904 (2018).
- [39] G. David, Event characterization in (very) asymmetric collisions, *J. Phys. Conf. Ser.* **589**, 012005 (2015).
- [40] C. Loizides and A. Morsch, Absence of jet quenching in peripheral nucleus-nucleus collisions, *Phys. Lett. B* **773**, 408 (2017).
- [41] S. Acharya *et al.* (ALICE Collaboration), Analysis of the apparent nuclear modification in peripheral Pb-Pb collisions at 5.02 TeV, *Phys. Lett. B* **793**, 420 (2019).
- [42] A. Bzdak, V. Skokov, and S. Bathe, Centrality dependence of high energy jets in p+Pb collisions at energies available at the CERN Large Hadron Collider, *Phys. Rev. C* **93**, 044901 (2016).

- [43] M. Alvioli and M. Strikman, Color fluctuation effects in proton-nucleus collisions, *Phys. Lett. B* **722**, 347 (2013).
- [44] M. Alvioli, B. A. Cole, L. Frankfurt, D. V. Perepelitsa, and M. Strikman, Evidence for x -dependent proton color fluctuations in pA collisions at the CERN Large Hadron Collider, *Phys. Rev. C* **93**, 011902(R) (2016).
- [45] D. McGlinchey, J. L. Nagle, and D. V. Perepelitsa, Consequences of high- x proton size fluctuations in small collision systems at $\sqrt{s_{NN}} = 200$ GeV, *Phys. Rev. C* **94**, 024915 (2016).
- [46] K. Reygers, Proposal to use the $\gamma^{\text{dir}}/\pi^0$ ratio to estimate hadron suppression in a model-independent way, https://www.uni-muenster.de/imperia/md/content/physik_kp/agwessels/thesis_db/agwessels/reygers_2004_habilitation.pdf (2004).
- [47] F. Arleo, K. J. Eskola, H. Paukkunen, and C. A. Salgado, Inclusive prompt photon production in nuclear collisions at RHIC and LHC, *J. High Energy Phys.* **04**, 055 (2011).
- [48] B.-W. Zhang and I. Vitev, Direct photon production in d+A and A+A collisions at RHIC, *Mod. Phys. Lett. A* **24**, 2649 (2009).
- [49] K. Adcox *et al.* (PHENIX Collaboration), PHENIX detector overview, *Nucl. Instrum. Methods Phys. Res., Sec. A* **499**, 469 (2003).
- [50] M. Allen *et al.*, PHENIX inner detectors, *Nucl. Instrum. Methods Phys. Res., Sec. A* **499**, 549 (2003).
- [51] L. Aphecetche *et al.*, PHENIX calorimeter, *Nucl. Instrum. Methods Phys. Res., Sec. A* **499**, 521 (2003).
- [52] A. Adare *et al.* (PHENIX Collaboration), Neutral pion production with respect to centrality and reaction plane in Au+Au collisions at $\sqrt{s_{NN}}=200$ GeV, *Phys. Rev. C* **87**, 034911 (2013).
- [53] R. Brun, F. Bruyant, F. Carminati, S. Giani, M. Maire, A. McPherson, G. Patrick, and L. Urban, GEANT Detector Description and Simulation Tool (1994), CERN-W5013, CERN-W-5013, W5013, W-5013.
- [54] Y. Ren and A. Drees, Examination of the universal behavior of the η -to- π^0 ratio in heavy-ion collisions, *Phys. Rev. C* **104**, 054902 (2021).
- [55] A. Adare *et al.* (PHENIX Collaboration), Centrality dependence of low-momentum direct-photon production in Au+Au collisions at $\sqrt{s_{NN}} = 200$ GeV, *Phys. Rev. C* **91**, 064904 (2015).
- [56] N. Ramasubramanian, *Validation of the Glauber model for centrality determination in small system collisions*, Ph.D. thesis, Stony Brook University (December, 2021).
- [57] See Supplemental Material at [URL will be inserted by publisher], which includes Refs. [60–62], for detailed explanations for the specialists on breakdown of the systematic uncertainties, their correlations and propagation, as well as cancellation in ratios.
- [58] A. Adare *et al.* (PHENIX Collaboration), Direct-Photon Production in $p+p$ Collisions at $\sqrt{s} = 200$ GeV at Midrapidity, *Phys. Rev. D* **86**, 072008 (2012).
- [59] A. Adare *et al.* (PHENIX Collaboration), Direct photon production in d +Au collisions at $\sqrt{s_{NN}} = 200$ GeV, *Phys. Rev. C* **87**, 054907 (2013).
- [60] M. R. Aguilar, Z. Chang, R. K. Elayavalli, R. Fatemi, Y. He, Y. Ji, D. Kalinkin, M. Kelsey, I. Mooney, and V. Verkest, PYTHIA8 underlying event tune for RHIC energies, *Phys. Rev. D* **105**, 016011 (2022).
- [61] A. Adare *et al.* (PHENIX Collaboration), Scaling properties of fractional momentum loss of high- p_T hadrons in nucleus-nucleus collisions at $\sqrt{s_{NN}}$ from 62.4 GeV to 2.76 TeV, *Phys. Rev. C* **93**, 024911 (2016).
- [62] S. Adler *et al.* (PHENIX Collaboration), PHENIX on-line and off-line computing, *Nucl. Instrum. Methods Phys. Res., Sec. A* **499**, 593 (2003).